JOURNAL OF GUIDANCE, CONTROL, AND DYNAMICS
Vol. 17, No. 5, September–October 1994

Nonlinear Approach to Aircraft Tracking Problem

Robert H. Bishop*
University of Texas at Austin, Austin, Texas 78712
and
A. C. Antoulas†
Rice University, Houston, Texas 77251

A nonlinear approach to the problem of tracking a maneuvering aircraft is presented. A nonlinear aircraft maneuver model is proposed for state estimation as well as prediction. The nonlinear model describes planar trajectories. A geometric nonlinear filter (GNF) is presented. The results show a significant overall improvement over the extended Kalman filter (EKF) approach. The GNF was found to be stable in most cases where the EKF was not stable. For the stable cases, the tracking performance of the GNF compares favorably with the EKF. The GNF offers a substantial savings in computational time.

I. Introduction

THIS paper deals with the problem of tracking a maneuvering aircraft. The approach presented here differs from previous work in the following areas: 1) the aircraft maneuver model and 2) the filter design method. The aircraft maneuver model, which is described in detail in Sec. II, is nonlinear and the three spatial directions are coupled. In much of the previous work,[1–9] evasive maneuvers were viewed as a response to a random perturbation. The perturbations were modeled as zero-mean, white Gaussian processes and as correlated random processes.[6] Berg[1] added a constant term to this acceleration model that he called an adaptive estimate of the mean target jerk. The maneuvers were also modeled as random processes whose mean values switch randomly from among a finite set of predefined values.[3–5]

The common denominator in each of the models just described is that the resulting maneuver model is linear. Also, the accelerations in the three spatial directions are uncoupled and the state noise is applied in inertial coordinates. The resulting tracking algorithm generally consists of three independent Kalman filters, one for each spatial direction, incorporating measurements of position. Other types of filters including constant-gain filters, $\alpha-\beta$, and $\alpha-\beta-\gamma$ have been proposed. Different variations of the above models include using a maneuver detection scheme and switching between several filters in response to maneuvers of varying strengths.[9] A comparison of these various filters can be found in Singer and Behnke.[7]

Improvements in the tracking performance can be achieved by incorporating attitude information in the tracking filters as well as position measurements. Kendrick et al.[10] originally proposed using attitude measurements to estimate the acceleration magnitude. Andrisani et al.[11,12] supplemented position measurements with attitude angles to enhance the tracking of aircraft and helicopters. In operations, the attitude information would be obtained through a remote sensing device or, if possible, by telemetry down-link from the vehicle.

The approach taken here begins with the development of a nonlinear maneuver model for the state estimation task. The nonlinear maneuver model is a more sophisticated alternative to the linear models just described. The resulting tracking filters are nonlinear and the three spatial disturbances are highly coupled. Perturbations to this maneuver model are modeled in the aircraft body frame as correlated random noise. The available measurements are assumed to be the position type only; no aircraft attitude information is available.

The nonlinear maneuver model is also utilized for the state prediction. Since the model describes planar trajectories, the number of first-order differential equations that must be integrated is reduced from nine to four, thus reducing the computational burden.

The basic idea of the design method presented here is to transform the nonlinear maneuver model to a linear form through the use of nonlinear state transformations so that the well-developed linear theory can be utilized in the filter gain calculations. The filter retains its nonlinear form. This filter design technique results in what will be referred to here as a geometric nonlinear filter (GNF). This approach has recently attracted much attention.[13–21] Central to the GNF approach is the transformation of the nonlinear system to a linear form, known as the observer canonical form, through the use of a nonlinear state transformation and output injection.

The question of the existence of transformations to observer canonical form has been addressed by Krener and Isidori,[18] Krener and Respondek,[19] and Phelps and Krener.[20] Assuming a transformation exists, Bestle and Zeitz[13] show how a GNF design can be accomplished without actually computing the transformation. Krener et al.[22] and Krener[17] introduced the modified and approximate observer canonical form and developed the asymptotic GNF technique. This technique accounts for state and measurement perturbations and results in a solution very similar in nature to the Kalman filter. Although it is desirable to have a system in observer canonical form, this is not always possible. The modified observer canonical form allows the injection term to include states that are not measured directly but that can be estimated quickly and accurately. With this new canonical form, the GNF approach can then be applied to a larger family of nonlinear systems. The approximate observer canonical form is used in the GNF design proposed here. Frezza et al.[14] applied the asymptotic GNF technique to a one-dimensional tracking problem with success. The tracking performance compared favorably to the extended Kalman filter (EKF) but at a substantial savings in computational time.

A GNF and an EKF are designed and evaluated in this paper. The GNF is stable for a much wider range of initial conditions than the EKF. Also, the GNF requires less computational time, yet tracks at least as well as the EKF. The performance evaluation is conducted utilizing simulated aircraft trajectories as well as "real-world" trajectories.

This paper is organized as follows: Section II presents the derivation of the aircraft maneuver model. Section III describes the GNF design procedure. Section IV describes the transformation of the aircraft maneuver model to approximate observer canonical form. The GNF design for the aircraft tracking problem is in Sec. V. The results and conclusions are presented in Secs. VI and VII, respectively.

II. Aircraft Maneuver Model

The assumptions leading to the nonlinear maneuver model are 1) the change in the aerodynamic lift and thrust-drag accelerations

Received Nov. 12, 1992; revision received Sept. 25, 1993; accepted for publication Nov. 13, 1993.

*Assistant Professor, Department of Aerospace Engineering and Engineering Mechanics. Senior Member AIAA.

†Associate Professor, Department of Electrical and Computer Engineering.

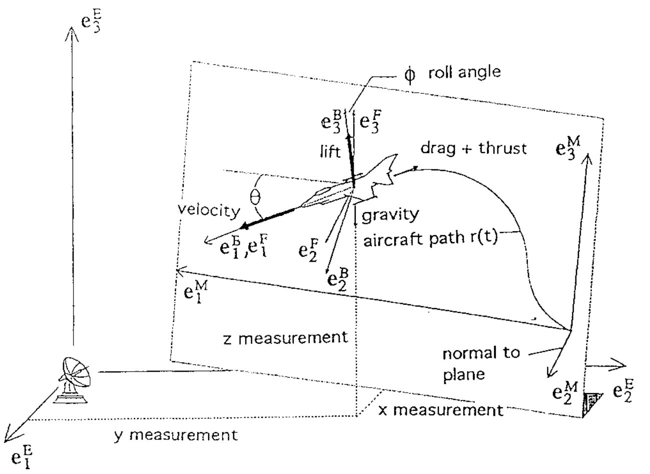

Fig. 1 Maneuver plane geometry.

is zero, 2) the aircraft body rate about the roll axis is zero, and 3) the angle of attack and sideslip are zero.

These assumptions reduce the problem of modeling the aircraft motion to a kinematics problem. There is no need to model the pilot response and also no need to estimate the aircraft angular attitude.

Letting $\boldsymbol{a}$ equal the sum of the aerodynamic and propulsive accelerations acting on the aircraft, by assumption 1,

$$\dot{\boldsymbol{a}}_B = 0 \tag{1}$$

It is assumed that the aerodynamic accelerations include only lift along $\boldsymbol{e}_3^B$ and drag along $\boldsymbol{e}_1^B$ (see Fig. 1). Aerodynamic accelerations along $\boldsymbol{e}_2^B$ are assumed to be zero. Assumption 2 implies that

$$\dot{\phi} = \omega^B \cdot \boldsymbol{e}_1^B = 0 \tag{2}$$

The aircraft angular velocity vector ω^B is computed by utilizing Poisson's formulas[23]:

$$\dot{\boldsymbol{e}}_i^B = \omega^B \times \boldsymbol{e}_i^B, \qquad i = 1, 2, 3$$

Forming the cross product $\boldsymbol{e}_i^B \times \dot{\boldsymbol{e}}_i^B$ and using the identity

$$\boldsymbol{v}_1 \times (\boldsymbol{v}_2 \times \boldsymbol{v}_3) = (\boldsymbol{v}_1 \cdot \boldsymbol{v}_3)\boldsymbol{v}_2 - (\boldsymbol{v}_1 \cdot \boldsymbol{v}_2)\boldsymbol{v}_3$$

the formula for ω^B is

$$\omega^B = (\omega^B \cdot \boldsymbol{e}_i^B)\boldsymbol{e}_i^B + \boldsymbol{e}_i^B \times \dot{\boldsymbol{e}}_i^B, \qquad i = 1, 2, 3 \tag{3}$$

By assumption 2, Eq. (3) reduces to

$$\omega^B = \boldsymbol{e}_1^B \times \dot{\boldsymbol{e}}_1^B \tag{4}$$

for the specific case where $i = 1$. Using assumption 3, it follows that

$$\boldsymbol{e}_{1E}^B = \frac{\dot{\boldsymbol{r}}_E}{\|\dot{\boldsymbol{r}}_E\|} \tag{5}$$

Equation (5) is differentiated with respect to time, and together with $\boldsymbol{e}_1^B \cdot \dot{\boldsymbol{e}}_1^B = 0$, it follows that

$$\dot{\boldsymbol{e}}_{1E}^B = \frac{\ddot{\boldsymbol{r}}_E}{\|\dot{\boldsymbol{r}}_E\|} - \left(\frac{\ddot{\boldsymbol{r}}_E \cdot \dot{\boldsymbol{r}}_E}{\|\dot{\boldsymbol{r}}_E\|^3}\right)\dot{\boldsymbol{r}}_E \tag{6}$$

Substituting Eqs. (5) and (6) into Eq. (4) yields

$$\omega_E^B = \frac{\dot{\boldsymbol{r}}_E \times \ddot{\boldsymbol{r}}_E}{\|\dot{\boldsymbol{r}}_E\|^2} \tag{7}$$

With respect to the inertial reference frame the accelerations acting on the aircraft are given by

$$\ddot{\boldsymbol{r}}_E = \boldsymbol{a}_E + \boldsymbol{g}_E \tag{8}$$

where $\boldsymbol{g}_E$ is the constant gravity acceleration in the inertial reference frame. With respect to the body reference frame, Eq. (8) becomes

$$\boldsymbol{L}_{BE}(\ddot{\boldsymbol{r}}_E - \boldsymbol{g}_E) = \boldsymbol{L}_{BE}\boldsymbol{a}_E = \boldsymbol{a}_B \tag{9}$$

where $\boldsymbol{L}_{BE}$ is a transformation matrix from inertial to body reference frame. Differentiating Eq. (9), using the fact that

$$\boldsymbol{L}_{EB}\dot{\boldsymbol{L}}_{BE}\boldsymbol{v}_E = -\omega_E^B \times \boldsymbol{v}_E \qquad \forall\, \boldsymbol{v}_E$$

and using assumption 1 and Eq. (7), yields the kinematic equation of motion

$$\dddot{\boldsymbol{r}}_E = \frac{\dot{\boldsymbol{r}}_E \times \ddot{\boldsymbol{r}}_E}{\|\dot{\boldsymbol{r}}_E\|^2} \times (\ddot{\boldsymbol{r}}_E - \boldsymbol{g}_E) \tag{10}$$

A condition on the aircraft trajectory is that the velocity $\|\dot{\boldsymbol{r}}_E\|$ must always be different from zero.

In this paper the radar measurement set is taken to be the aircraft inertial position vector $\boldsymbol{r}_E$ in Cartesian coordinates. This leads to a linear measurement model. The (noise-free) measurement equation is

$$\boldsymbol{y} = \boldsymbol{r}_E \tag{11}$$

If the state vector $\boldsymbol{x}$ is defined as

$$x_{3i-2} = r_i, \quad x_{3i-1} = \dot{r}_i, \quad x_{3i} = \ddot{r}_i \qquad i = 1, 2, 3 \tag{12}$$

then the aircraft maneuver model Eq. (10) can be written as

$$\dot{\boldsymbol{x}} = \boldsymbol{f}(\boldsymbol{x}), \qquad \boldsymbol{y} = \boldsymbol{h}(\boldsymbol{x}) \tag{13}$$

A check shows that Eq. (13) is an observable system.

When viewed as an arbitrary speed space curve, the aircraft trajectory $\boldsymbol{r}(t)$ has zero torsion. Thus, the aircraft maneuver model describes planar trajectories in a maneuver plane (see Fig. 1). The curvature, on the other hand, is in general not zero. The maneuver reference frame can be taken to be the Frenet[24] reference frame at t_0. The aircraft roll angle ϕ is assumed to be a constant. The relevant transformation matrices are the inertial to maneuver plane, $\boldsymbol{L}_{ME}$, and the body to inertial, $\boldsymbol{L}_{EB}$.

In the maneuver plane the trajectory is described by

$$\begin{aligned} \dot{v} &= -g_{mz}\sin\theta + g_{mx}\cos\theta + c_1 \\ v\dot{\theta} &= -g_{mz}\cos\theta - g_{mx}\sin\theta + c_2 \\ \dot{c}_1 &= 0 \\ \dot{c}_2 &= 0 \end{aligned} \tag{14}$$

The constant c_1 is the sum of the thrust and drag accelerations. The constant c_2 is the lift acceleration times the cosine of the roll angle, v is the velocity magnitude, and $\boldsymbol{g}_m$ is the constant gravity vector in the maneuver plane. Once an inertial state estimate is available, the matrix $\boldsymbol{L}_{ME}$ can be computed and the four equations in Eq. (14) can be used for state prediction. This prediction scheme was used successfully by Berg.[1]

III. Geometric Nonlinear Filter Design

Considered in this paper are nonlinear filters of the form (Kou et al.[25] and Thau[26])

$$\dot{\hat{\boldsymbol{x}}} = \boldsymbol{f}(\hat{\boldsymbol{x}}) + \boldsymbol{K}^*(\hat{\boldsymbol{x}})[\boldsymbol{y} - \boldsymbol{h}(\hat{\boldsymbol{x}})] \tag{15}$$

In the GNF design proposed here, $\boldsymbol{K}^*(\hat{\boldsymbol{x}})$ is computed to guarantee stability of the estimation error. As in the EKF, the GNF gains are state dependent, although the state dependency manifests itself through algebraic manipulations rather than through the on-line integration of a state-dependent matrix differential equation. The GNF design lends itself to computer implementation and the computational burden is very low relative to the EKF.

The GNF design includes the following four steps.

Step 1: The first step in the GNF design process is to find a (bijective) C^∞ transformation $T: R^n \to R^n$ that transforms the state x to z;

$$x = T(z) \tag{16}$$

in such a way that the system in Eq. (13) is transformed into observer canonical form

$$\dot{z} = Az + b(Cz), \qquad y = Cz$$

where A and C are in Brunovsky form. The main characteristics of the observer canonical form are that the output is linear in the state and that the (nonlinear) output injection term depends only on states that are measured. The advantage of this form over the original nonlinear form is that the process of computing the filter gains to ensure stability of the estimation error is simplified. When a transformation to observer canonical form exists, a general theory exists for designing a stable filter.[13]

Not all nonlinear systems can be brought to observer canonical form through use of a nonlinear transformation with output injection. The aircraft maneuver model cannot be transformed to observer canonical form. It can be transformed to approximate observer canonical form

$$\dot{z} = Az + b(z), \qquad y = Cz$$

in which $b(z)$ is approximately zero for small turn rates and

$$\lim_{\|z-\hat{z}\|\to 0} \frac{\tilde{b}(z, \hat{z})}{\|z-\hat{z}\|} \to 0$$

where

$$b(z) = b(\hat{z}) - B(\hat{z})e_z - \tilde{b}(z, \hat{z})$$

and

$$B(\hat{z}) = \left.\frac{\partial b}{\partial z}\right|_{z=\hat{z}}$$

Consider a transformation, as in Eq. (16), such that Eq. (13) is transformed to approximate observer canonical coordinates. Then the filter equation (15) is transformed to

$$\dot{\hat{z}} = A\hat{z} + b(\hat{z}) + J(\hat{z})^{-1}K^*(\hat{z})(y - C\hat{z})$$

where $J(\hat{z})$ is the Jacobian of the transformation. Define the time-varying, nonlinear gain

$$K(\hat{z}) := J(\hat{z})^{-1}K^*(\hat{z}) \tag{17}$$

and the approximate observer canonical form estimation error

$$e_z := \hat{z} - z \tag{18}$$

Then the estimation error is described by the differential equation

$$\dot{e}_z = [A - K(\hat{z})C]e_z + b(\hat{z}) - b(z) \tag{19}$$

Linearizing $b(z)$ about the estimated trajectory $\hat{z}$ using a Taylor series expansion yields

$$\dot{e}_z = A^*(\hat{z})e_z + \tilde{b}(z, \hat{z}) \tag{20}$$

where

$$A^*(\hat{z}) = A - K(\hat{z})C + B(\hat{z})$$

The goal of the GNF design is to compute $K(\hat{z})$ such that the estimation error described by Eq. (20) is stable.

Step 2: The second step is to compute $K(\hat{z})$ such that the desired eigenvalues of $A^*(\hat{z})$ are achieved for all $t \geq t_0$. Since asymptotic stability is not ensured by the fact that all the eigenvalues of $A^*(\hat{z})$ have negative real parts, the time variation of $A^*(\hat{z})$ must be accounted for in the stability analysis. This generally leads to a slowly time-varying condition for stability.

Step 3: The gain $K(\hat{z})$ must be chosen so that the estimation error asymptotically approaches zero when the nonlinear term $\tilde{b}(z, \hat{z})$ is accounted for. The sufficient conditions to guarantee asymptotic stability in the presence of nonzero $\tilde{b}(z, \hat{z})$ can be obtained through the application of Lyapunov's indirect method. Explicit conditions have been obtained for the aircraft tracking problem.[27]

Step 4: The final step in the design process is to compute $K^*(\hat{z})$ via

$$K^*(\hat{z}) = J(\hat{z})K(\hat{z})$$

Stability of e_z implies stability of e_x since T is continuous.

IV. Approximate Observer Canonical Form

A nonlinear transformation that transforms the aircraft maneuver model to approximate observer canonical form is

$$x = T(z) \tag{21}$$

where

$$\begin{aligned} x_{3i-2} &= n_{i1}z_1 + (n_{i2}\cos\phi + n_{i3}\sin\phi)z_4 \\ &\quad + (-n_{i2}\sin\phi + n_{i3}\cos\phi)z_7 \\ x_{3i-1} &= n_{i1}z_2 + (n_{i2}\cos\phi + n_{i3}\sin\phi)z_5 \\ &\quad + (-n_{i2}\sin\phi + n_{i3}\cos\phi)z_8 \\ x_{3i} &= \{(n_{i1}z_2 + n_{i3}\bar{z})(z_3 - g_1) + [(n_{i3}z_2 + n_{i1}\bar{z})\sin\phi \\ &\quad + n_{i2}\Delta\cos\phi](z_6 - g_2) - [(n_{i3}z_2 - n_{i1}\bar{z})\cos\phi \\ &\quad + n_{i2}\Delta\sin\phi](z_9 - g_3)\}/\Delta \end{aligned}$$

where $i = 1, 2, 3$ and ϕ is the aircraft roll angle (assumed constant in the maneuver model), the constant terms n_{ij} are the (i, j)th elements of L_{EM}, and

$$\bar{z} = z_8\cos\phi + z_5\sin\phi, \qquad \Delta = \sqrt{z_2^2 + \bar{z}^2}$$

The nonzero elements of the residual nonlinear terms are

$$b_2(z) = (z_3 - g_1)(\cos\theta - 1) - \tilde{z}\sin\theta$$

$$b_5(z) = [(z_3 - g_1)\sin\theta + \tilde{z}(\cos\theta - 1)]\sin\phi$$

$$b_8(z) = [(z_3 - g_1)\sin\theta + \tilde{z}(\cos\theta - 1)]\cos\phi$$

where

$$\tilde{z} = (z_6 - g_2)\sin\phi + (z_9 - g_3)\cos\phi$$

$$\cos\theta = z_2/\Delta, \qquad \sin\theta = -\bar{z}/\Delta$$

and

$$g_1 = n_{31}g, \quad g_2 = (n_{32}\cos\phi + n_{33}\sin\phi)g$$

$$g_3 = (n_{33}\cos\phi - n_{32}\sin\phi)g$$

One characteristic of $b(z)$ is that, when $\theta = 0$, $b(z) = 0$ and the system is exactly linear and in observer canonical form. For small turn rates, $\theta \approx 0$, it follows that $b(z) \approx 0$ and the system is approximately in observer canonical form, hence the label "approximate observer canonical form."

V. Geometric Nonlinear Filter Gain Calculation

In this section, a method for arbitrarily placing the poles of $A^*(\hat{z})$ in Eq. (20) is presented. This is of interest because, when $\tilde{b}(z, \hat{z}) = 0$, the error equation reduces to

$$\dot{e}_z = A^*(\hat{z})e_z \tag{22}$$

In practice, the system disturbances and the higher order terms cannot be neglected. However, the gain matrix derived by first considering Eq. (22) serves as the starting point. The effect of nonzero system disturbances and $\tilde{b}(z, \hat{z}) \neq 0$ must then be investigated.

The specific multi-output situation considered here has 12 states and 3 outputs, and the observability indices are $l_1 = l_2 = l_3 = 4$. This case represents the maneuvering aircraft tracking problem described in the previous sections. The extension to other multi-output situations follows the same patterns established here. In the multi-output case, the matrices A and C are in block Brunovsky form. The construction of the stabilizing gain $K(\hat{z})$ depends on the five matrices $\bar{\Theta}(\hat{z})$, $Q_a(\hat{z})$, $R(\hat{z})$, $B_1(\hat{z})$, $J(\hat{z})$. The matrix $B_1(\hat{z})$ is defined as

$$B_1(\hat{z}) := B(\hat{z})C^T$$

Associated with $B_1(\hat{z})$ we have

$$B^*(\hat{z}) = B(\hat{z}) - B_1(\hat{z})C = B(\hat{z})(\mathbf{I} - C^T C)$$

Utilizing the above definition of $\mathbf{B}^*(\hat{z})$, the matrix $\bar{\Theta}(\hat{z})$ is defined as the observability matrix associated with $(C, A + B^*(\hat{z}))$. The main assumption used in the sequel is rank $\bar{\Theta}(\hat{z}) = n, \forall t \geq t_0$. In the multi-output case considered here, we have

$$\begin{aligned} C[A + B^*(\hat{z})]^4 = {} & [a_{1jk}(\hat{z})]\{C[A + B^*(\hat{z})]\} \\ & + [\mathbf{a}_{2jk}(\hat{z})]\{C[A + B^*(\hat{z})]^2\} \\ & + [\mathbf{a}_{3jk}(\hat{z})]\{C[A + B^*(\hat{z})]^3\} \end{aligned}$$

where $[a_{ijk}(\hat{z})]$ are 3×3 matrices. Since, by assumption, the rank $\bar{\Theta}(t) = n = 12$, $\forall t \geq t_0$, the matrices $[a_{ijk}(\hat{z})]$ exist. The matrix $Q_a(\hat{z})$ is defined as

$$Q_a(\hat{z}) := \begin{bmatrix} Q_{a11}(\hat{z}) & Q_{a12}(\hat{z}) & Q_{a13}(\hat{z}) \\ Q_{a21}(\hat{z}) & Q_{a22}(\hat{z}) & Q_{a23}(\hat{z}) \\ Q_{a31}(\hat{z}) & \mathbf{Q}_{a32}(\hat{z}) & Q_{a33}(\hat{z}) \end{bmatrix}$$

where

$$Q_{aii}(\hat{z}) = \begin{bmatrix} 1 & 0 & 0 & 0 \\ -a_{ii3} & 1 & 0 & 0 \\ -a_{ii2} & -a_{ii3} & 1 & 0 \\ -a_{ii1} & -a_{ii2} & -a_{ii3} & 1 \end{bmatrix}$$

and

$$Q_{aij}(\hat{z}) = \begin{bmatrix} 0 & 0 & 0 & 0 \\ -a_{ji3} & 0 & 0 & 0 \\ -a_{ji2} & -a_{ji3} & 0 & 0 \\ -a_{ji1} & -a_{ji2} & -a_{ji3} & 0 \end{bmatrix} \qquad \text{for } i \neq j$$

The matrix $R(\hat{z})$ is

$$R(\hat{z}) := \begin{bmatrix} R_{11}(\hat{z}) \\ R_{21}(\hat{z}) \\ R_{31}(\hat{z}) \end{bmatrix}$$

where

$$R_{i1}(\hat{z}) = \begin{bmatrix} -a_{1i3} & -a_{2i3} & -a_{3i3} \\ -a_{1i2} & -a_{2i2} & -a_{3i2} \\ -a_{1i1} & -a_{2i1} & -a_{3i1} \\ 0 & 0 & 0 \end{bmatrix}$$

With the above definitions, we have the following theorem for the case of 3 outputs, 12 states, and observability indices $l_1 = l_2 = l_3 = 4$.

Theorem 1. Suppose that the desired characteristic polynomial of $A^*(\hat{z})$ is

$$\rho_{\text{des}} = \prod s^4 + \rho_{4i-3,i}s^3 + \rho_{4i-2,i}s^2 + \rho_{4i-1,i}s + \rho_{4i,i} \qquad \text{for } i = 1, 2, 3$$

Associated with the desired characteristic polynomial, define the block-diagonal matrix $K_1 = \operatorname{diag}(K_{11}, K_{22}, K_{33})$ with

$$K_{ii} = [\rho_{4i-3,i} \quad \rho_{4i-2,i} \quad \rho_{4i-1,i} \quad \rho_{4i,i}]^T$$

If

$$K(\hat{z}) = B_1(\hat{z}) + Q^{-1}(\hat{z})[K_1 + R(\hat{z})]$$

where

$$Q(\hat{z}) = Q_a(\hat{z})\bar{\Theta}(\hat{z})$$

then it follows that the characteristic polynomial of $A^*(\hat{z})$ is ρ_{des}. Also,

$$A^*(\hat{z}) = A - K(\hat{z})C + B(\hat{z}) = Q^{-1}(\hat{z})(A - K_1 C)Q(\hat{z})$$

Proof. The proof follows from the facts that $CQ^{-1} = C$ and $Q(\hat{z})[A + B^*(\hat{z})] + R(\hat{z})\, C = AQ(\hat{z})$.

VI. Aircraft Tracking Results

The GNF design proposed in the previous sections is tested here. The tests are based on two types of measurement data. The first type of measurement data is generated by simulation of the aircraft maneuver model. A more detailed analysis of the filter is possible since all parameters of the problem (i.e., initial state errors, state and measurement noise values) can be controlled. The second type of measurement data is from 26 aircraft maneuvers. Using actual radar measurements, the good tracking performance of the GNF in a real-world environment is verified.

The aircraft maneuver model was developed on the assumptions that the time variation of the roll angle is zero and the time variation of the aerodynamic and propulsive accelerations is zero. The state perturbations used in the simulations and in the EKF development follow directly from these assumptions.

The perturbation in the time variation of the aerodynamic and propulsive accelerations, naturally modeled in the aircraft body reference frame, is modeled by a random process in the thrust-drag direction, e_1^B, and in the lift direction, e_3^B. The uncertainty in the time variation of the roll angle is modeled by assuming that the time variation in $\dot{\phi}$ is random. It then follows from Eqs. (2), (3), and (10) that the uncertainty with respect to the inertial reference frame due to the roll rate uncertainty acts along the e_2^B axis. Since (z_3, z_6, z_9) is the acceleration in the body axis and the state perturbation u_z, is given in the body frame, the aircraft maneuver model (with perturbations) is given by

$$\dot{z} = Az + b(z) + u_z$$

The measurement uncertainties u_m, add directly to the measurements yielding

$$y = Cz + u_m$$

The model chosen here for the state perturbation is a first-order Gauss-Markov stochastic process. The measurement perturbation is modeled as a white Gaussian stochastic process. In the EKF method, the perturbations are accounted for via the standard EKF equations with state vector augmentation. In the GNF method proposed here, the expected magnitude of the perturbations are used to downweight the gains (off-line) and are not explicitly used on-line.

If the original system is modeled as a nonlinear stochastic system, then one must be careful when applying the transformation to observer canonical form.[28] In this aircraft tracking application, the perturbations are considered after the transformation since they are more naturally described with respect to the transformed states. The magnitude of the perturbations were adjusted so that the output of the model approximated the actual aircraft trajectories. The GNF can be viewed as an observer wherein the gains are downweighted (off-line) to account for the expected magnitude of the perturbations.

The first step is to choose the gains K_1 for stability. Recall that the aircraft maneuver model can be written in approximate observer canonical form such that when the aircraft turn rate in the maneuver plane is zero (i.e., $\theta = 0$), $b(z) = 0$ and the transformed system is a linear system. It is then possible to compute the optimal Kalman gains for the linear system off-line. The approach here is to use the steady-state Kalman gains (modified

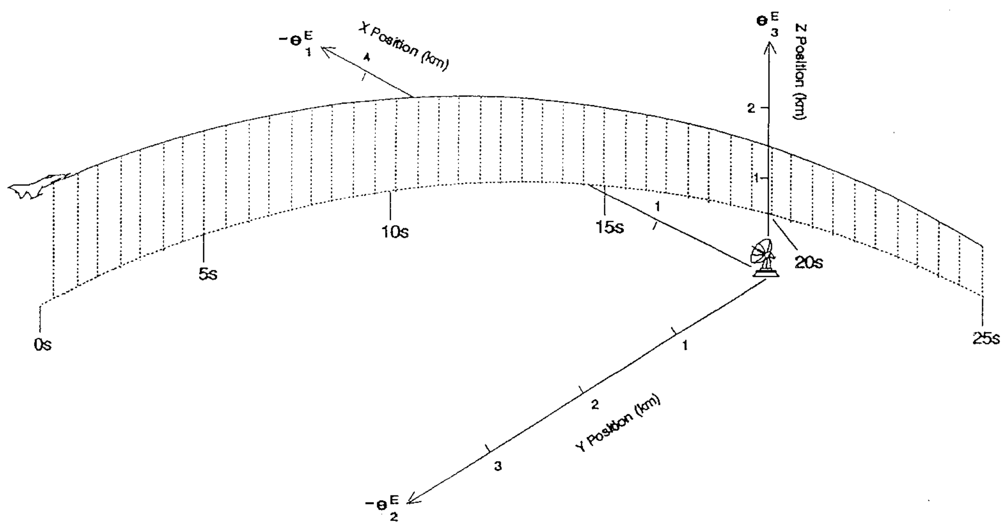

Fig. 2 Simulated nominal trajectory.

and tuned slightly for better performance in maneuvers) as $\boldsymbol{K}_1$. In maneuvering situations these gains provide stability of the estimation error but are not optimal. They also provide a good trade-off between the desire to speed up the convergence of the estimation error by using large gains and the desire to eliminate the effects of the measurement and state noise by using small gains. The filter initial loads used to compute the steady-state Kalman gains $\boldsymbol{K}_1$ are also used as the EKF initial filter loads.

A. Comparison Based on Simulated Aircraft Trajectories

The effects on the tracking performance of the GNF and the EKF with initial state errors and measurement noise are investigated here. The simulation results of this section are based on the nominal trajectory in Fig. 2.

The first study involved the stability of both filters for initial state error stress cases. For example, when the initial state errors are (−600.0, 10.0, 30.0) (meters) for position, (−23.0, 0.0, −1.0) (meters per square second) for velocity, and (0.0, −9.806, 0.0) (meters per square second) for acceleration, then the EKF is unstable, whereas the GNF is not only stable but the tracking performance is good. These particular initial state errors represent a realistic but stressful situation for both filters. Other simulation results show that the GNF will converge with most realistic initial state errors, even those well outside of the domain of attraction. On the other hand, unstable initial conditions for the EKF can be easily generated.

To investigate the stability characteristics of the filters initialized with nominal and near-nominal initial state errors, 100 state 1σ, 2σ, and 3σ errors were generated from the initial covariance matrix. Both filters tracked these trajectories successfully. This shows that when the EKF is initialized with initial state errors at or near its design values, it will converge.

The effects of varying levels of measurement noise on the tracking performance are investigated by considering the 1σ, 2σ, and 3σ values of the measurement noise covariance, where the 1σ value is 1.0 m. In all the simulation runs, the 1σ value of the state noise was used. For each level of measurement noise, 100 runs were made, with each run corresponding to a different trial of the state and measurement noise processes. This process was repeated for the 2σ and 3σ cases.

The scalar performance measure is the percentage of time that the projected (1-s-ahead) position error was less than 5 and 10 m. This was calculated and averaged over the 100 runs. A higher percentage implies better performance. The results are shown in Fig. 3. They show that both filters perform quite well and the results are quite similar. The performance degrades as the noise level increases, as expected. The trends indicate that the GNF performs as well or better than the EKF near the design point ($\sigma_m^2 = 1, 4$) but tends

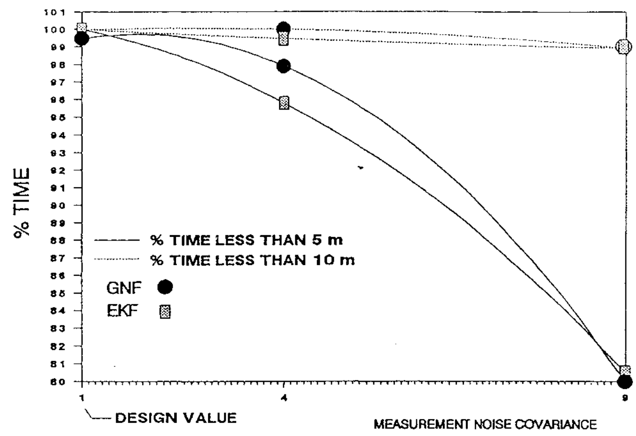

Fig. 3 Performance with measurement noise.

to drop off faster than the EKF as the noise increases ($\sigma_m^2 = 9$). Thus, for very large measurement noises, the EKF will perform better. From a tracking performance point of view, both filters have approximately the same performance for different expected levels of measurement noise, yet the GNF takes about 10 times less CPU time.

B. Comparison Based on Actual Aircraft Trajectories

The performance of the two filters in a "real-world" environment is investigated by processing actual radar measurement data in both the GNF and the EKF. An example of an actual aircraft trajectory is shown in Fig. 4. Traj A contains 4 roll maneuvers, occurring approximately at 2, 15, 24, and 36 s. Between the discrete roll maneuvers, the trajectories are described very accurately by the aircraft maneuver model, thus justifying the proposed nonlinear model.

The tracking performance for Traj A is shown in Fig. 5. The first noticeable characteristic is that the GNF and EKF performances are similar. This also turns out to be the case for the remaining 25 trajectories.

The roll maneuvers show up as increased errors. In Fig. 5, it can be seen that two roll maneuvers result in increased errors in the X direction and the remaining two roll maneuvers result in increased errors in the Y direction. Between the roll maneuvers the errors are less than 15 m. The errors in the Z direction (not shown) are small and uneventful since the aircraft is exhibiting very little motion in that direction.

To compare the GNF and EKF, a performance index π is defined as the average (over all 26 trajectories) of the predicted (1-s-ahead)

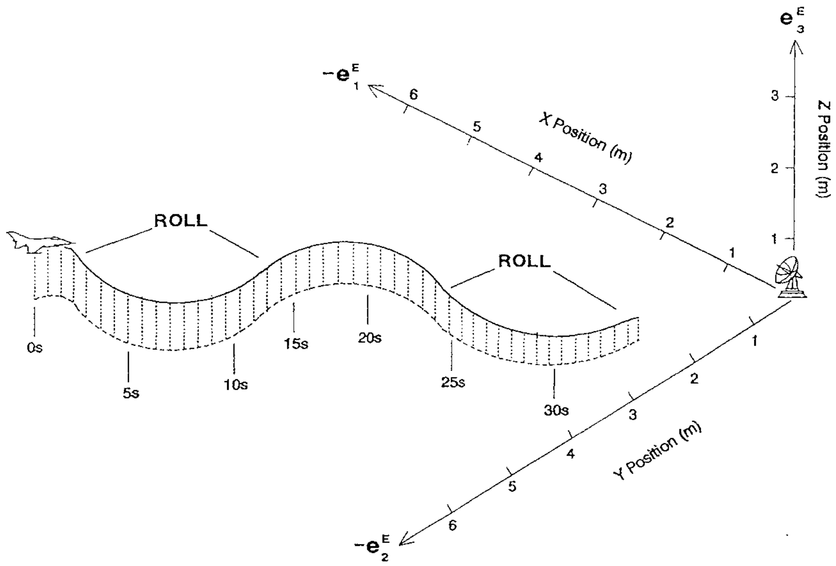

Fig. 4 Example aircraft trajectory, Traj A.

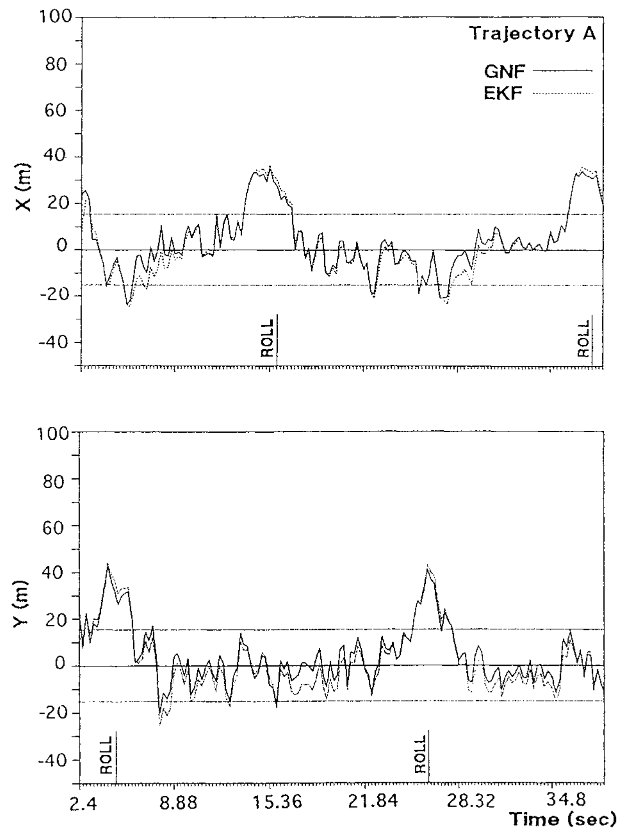

Fig. 5 Traj A tracking errors predicted 1-s-ahead.

position error squared. The results show that

$$\pi(\text{GNF}) = 376.3, \qquad \pi(\text{EKF}) = 412.7$$

Thus, for these particular test cases, the GNF performed better.

VII. Conclusions

The nonlinear aircraft maneuver model and the GNF design approach are promising alternatives to the linear approaches based on random perturbation accelerations and to the nonlinear approach of the EKF. The GNF has been shown to be effective in tracking real-world aircraft trajectories. It has performance at least as good as the EKF, but with an order-of-magnitude reduction in CPU time.

The performance of both filters would be improved by application of a roll maneuver detection scheme. This is not investigated in this paper but is a good topic for future research. Another topic for further research is the development of optimal gains for the GNF and the elimination of the slowly time-varying condition for stability.

Acknowledgments

The authors thank Heinz Piccolruaz and Jürg Weilenmann of Contraves Ltd., Zürich, for suggesting this problem and for their input.

References

[1]Berg, R. F., "Estimation and Prediction for Maneuvering Target Trajectories," *IEEE Transactions on Automatic Control*, Vol. 28, No. 3, 1983, pp. 303–313.

[2]Chang, C. B., and Tabaczynski, J. A., "Application of State Estimation to Target Tracking," *IEEE Transactions on Automatic Control*, Vol. 29, No. 2, 1984, pp. 98–109.

[3]Gholson, N. H., and Moose, R. L., " Maneuvering Target Tracking Using Adaptive State Estimation," *IEEE Transactions on Aerospace and Electronic Systems*, Vol. 13, No. 3, 1977, pp. 310–317.

[4]Moose, R. L., "Adaptive Estimator for Passive Range and Depth Determination of a Maneuvering Target(U)," *U.S. Naval Journal of Underwater Acoustics*, July 1973.

[5]Moose, R. L., Vanlandingham, H. F., and McCabe, D. H., "Modeling and Estimation for Tracking Maneuvering Targets," *IEEE Transactions on Aerospace and Electronic Systems*, Vol. 15, No. 3, 1979, pp. 448–456.

[6]Singer, R. A., "Estimating Optimal Tracking Filter Performance for Manned Maneuvering Targets," *IEEE Transactions on Aerospace and Electronic Systems*, Vol. 6, No. 4, 1970, pp. 420–436.

[7]Singer, R. A., and Behnke, K. W., "Real-Time Tracking Filter Evaluation and Selection for Tactical Applications," *IEEE Transactions on Aerospace and Electronic Systems*, Vol. 7, No. 1, 1971, pp. 100–110.

[8]Thorp, J. S., "Optimal Tracking of Maneuvering Targets," *IEEE Transactions on Aerospace and Electronic Systems*, Vol. 9, No. 4, 1973, pp. 512–519.

[9]Williams, D. E., and Friedland, B., "Target Maneuver Detection and Estimation," *Proceedings of the 27th Conference on Decision and Control*, WP13-4:30, Austin, TX, Dec. 1988, pp. 851–855.

[10]Kendrick, J. D., Maybeck, P. S., and Reid, J. G., "Estimation of Aircraft Target Motion Using Orientation Measurements," *IEEE Transactions on Aerospace and Electronic Systems*, Vol. 9, No. 2, 1973, pp. 254–259.

[11]Andrisani, D., Kuhl, F., and Gleason, D., "A Nonlinear Tracker Using Attitude Measurements," *IEEE Transactions on Aerospace and Electronic Systems*, Vol. 22, No. 5, 1986, pp. 533–538.

[12]Andrisani, D., Kim, E. T., and Schierman, J., "A Nonlinear Helicopter Tracker Using Attitude Measurements," *IEEE Transactions on Aerospace and Electronic Systems*, Vol. 27, No. 1, 1991, pp. 40–47.

[13]Bestle, D., and Zeitz, M., "Canonical Form Observer Design for Nonlinear Time-Variable Systems," *International Journal of Control*, Vol. 38,

No. 2, 1983, pp. 419–431.

[14]Frezza, R., Karahan, S., Krener, A. J., and Hubbard, M., "Application of an Efficient Nonlinear Filter," *Analysis and Control of Nonlinear Systems*, edited by C. I. Byrnes, C. F. Martin, and R. E. Sacks, Elsevier Science, North-Holland, Amsterdam, 1988, pp. 223–237.

[15]Hermann, R., and Krener, A. J., "Nonlinear Controllability and Observability," *IEEE Transactions on Automatic Control*, Vol. 22, No. 5, 1977, pp. 728–740.

[16]Hunt, L. R., Luksic, M., and Su, R., "Exact Linearizations of Input-Output Systems," *International Journal of Control*, Vol. 43, No. 1, 1986, pp. 247–255.

[17]Krener, A. J., "The Asymptotic Approximation of Nonlinear Filters by Linear Filters," *Theory and Applications of Nonlinear Control Systems*, edited by C. I. Byrnes and A. Lindquist, Elsevier Science, North-Holland, Amsterdam, 1986, pp. 359–378.

[18]Krener, A. J., and Isidori, A., "Linearization by Output Injection and Non-Linear Observers," *Systems and Control Letters*, Vol. 3, No. 1, 1983, pp. 47–52.

[19]Krener, A. J., and Respondek, W., "Nonlinear Observers with Linearizable Error Dynamics," *SIAM Journal of Control and Optimization*, Vol. 23, No. 2, 1985, pp. 197–215.

[20]Phelps, A. R., and Krener, A. J., "Computation of Observer Normal Form Using Macsyma," *Analysis and Control of Nonlinear Systems*, edited by C. I. Byrnes, C. F. Martin, and R. E. Sacks, Elsevier Science, North-Holland, Amsterdam, 1988.

[21]Walcott, B. L., Corless, M. J., and Zäk, S. H., "Comparative Study of Non-Linear State-Observation Techniques," *International Journal of Control*, Vol. 45, No. 6, 1987, pp. 2109–2132.

[22]Krener, A. J., Karahan, S., and Hubbard, M., "Approximate Normal Forms of Nonlinear Systems," *IEEE* Proceedings of the 27th Conference on Decision and Control.

[23]Miele, A., *Flight Mechanics*, Vol. 1: *Theory of Flight Paths*, Addison-Wesley, Reading, MA, 1962.

[24]O'Neill, B., *Elementary Differential Geometry*, Academic, New York, 1966.

[25]Kou, S. R., Elliott, D. L., and Tarn, T. J., "Exponential Observers for Non-Linear Dynamic Systems," *Information and Control*, Vol . 29, 1975, pp. 204–216.

[26]Thau, F. E., "Observing the State of Non-Linear Dynamic Systems," *International Journal of Control*, Vol. 17, No. 3, 1973, pp. 471–479.

[27]Bishop, R. H., "Geometric Non-linear Filtering Theory with Applications to the Maneuvering Tracking Problem," Ph.D. Dissertation, Rice University, Houston, TX, 1990.

[28]Mortensen, R. E., "Mathematical Problems of Modeling Stochastic Nonlinear Dynamic Systems," *Journal of Statistical Physics*, Vol. 1, No. 2, 1969, pp. 271–296.